Infrared Absorption Properties of Carbon Nanotube/Nanodiamond Based Thin Film Coatings

Vikrant Jayant Gokhale, *Student Member, IEEE*, Olga A. Shenderova, Gary E. McGuire, and Mina Rais-Zadeh, *Senior Member, IEEE*

***Abstract*— We report on the characterization of thin-film near and short wavelength infrared absorbers comprised of carbon nanotubes dispersed in a polymer. Charged nanodiamond particles are used to effectively and uniformly disperse the carbon nanotubes in the polymer matrix, leading to a very homogenous film. Using this new technique, we demonstrate an infrared absorption of up to 95% in films with thicknesses < 2000 nm. This remarkably high absorption is the result of low reflection off the surface and high absorption across the film thickness. The complex refractive index of the films is extracted using an effective media approximation. Calculations show the film has a wide angle for high absorption and is polarization independent. These films are easy to fabricate, robust and damage-resistant, and are compatible with post-processing techniques. These films can be used as the coating layer to boost the efficiency of uncooled infrared sensors and solar-thermal energy harvesters. [2013-0117]**

***Index Terms*— Carbon nanotubes, nanodiamonds, infrared sensor, thin films, coating.**

I. Introduction

THIN film coatings and optical metamaterials with engineered absorption, transmission, or reflection properties are critical components of numerous optical devices and systems, including infrared (IR) detectors, filters, modulators, radiation absorbing layers, and energy harvesters [1]–[4]. Specifically for thermal IR detectors, thin film coatings are needed that provide efficient absorption of incident radiation and convert it into thermal energy [5]–[8]. The generated heat is then transduced to other usable forms of energy (*e.g.* electrical energy) using other materials in contact with the absorber. This principle forms the basis of many thermal detectors, including thermocouples, bolometers, pyroelectric and resonant detectors [5], [6]. Absorber layers for IR detectors require the following attributes [8]: (i) high and polarization independent absorption [2], (ii) low thermal and inertial mass, (iii) good thermal conductivity, (iv) stable and reproducible properties, and (v) manufacturable using a process compatible with detector and electronics fabrication technologies. Similarly, for solar-thermal energy harvesting, a material is required that is an efficient absorber across a broad spectrum ranging from visible to at least near-IR [9].

Popular solutions that meet some of these requirements include thin metal films, resonant cavity structures, plasmonic metamaterials, and porous surfaces. However, ultra-thin metal films are limited in terms of absolute absorbance and are not temperature stable [11]. Porous films and metal-blacks require well controlled etch chemistry and suffer from temperature instability [12]. Surface plasmonic resonances (SPR) and quarter wavelength cavity resonances are good solutions for selective detection with spectral bandwidths on the order of 10% or lower in the visible-IR range, but need precise control of design and fabrication to achieve this goal [2], [8]. Extending these mechanisms to broadband absorption is difficult [13]. Another more recent method utilizes vertically aligned arrays of carbon nanotubes (CNTs) as broadband visible/IR absorbers [1], [4], [14]. The principle of absorption here is based on trapping light in the sparse and tall CNT arrays. The sparsity enables very close matching of the refractive index to that of free space/air. The height of the arrays (tens to hundreds of microns) allows for multiple internal reflections and the eventual absorption of all incident radiation over a large spectral range. While the measured absorption of these arrays is excellent [14], the drawback of this approach is their large mass and thermal loading on the detector. In addition, the high temperatures and catalytic surfaces required for vertical CNT arrays, the precise sub-micron lithography required for SPR absorbers, and the etch chemistry control required for porous metal and metal-black films make these methods prohibitive for economical, large scale fabrication.

In this work, we present a thin film material [15] that has a refractive index $\boldsymbol{n}$ close to unity and a high extinction coefficient $\boldsymbol{k}$ at near infrared (NIR) and short wavelength infrared (SWIR) range. The absorber is thin and light so that the transducer is not significantly loaded mechanically or thermally. The film is easy to fabricate on any surface, and at low manufacturing cost. The measured absorption is as high as 95% over a broad spectral range. The absorber material comprises of a mixture of multiwalled CNTs and detonation nanodiamond (DND) particles suspended in a polymer matrix. This material offers markedly high absorption efficiency per unit thickness over a broad range in the NIR/SWIR spectrum, making it an ideal candidate for use in applications requiring low-profile coatings. The low cost, ease of manufacturability,

Manuscript received April 15, 2013; revised May 22, 2013; accepted May 26, 2013. This work was supported in part by the National Science Foundation under Grant 1002036 and in part by the Army Research Laboratory under Contract W911NF and prepared through participation in the MAST CTA. Subject Editor S. Merlo.

V. J. Gokhale and M. Rais-Zadeh are with the Department of Electrical Engineering and Computer Science, University of Michigan, Ann Arbor, MI 48109 USA (e-mail: vikrantg@umich.edu; minar@umich.edu).

O. A. Shenderova and G. E McGuire are with the International Technology Center, Raleigh, NC 27617 USA (e-mail: oshenderova@itc-inc.org; gmcguire@itc-inc.org).

Color versions of one or more of the figures in this paper are available online at http://ieeexplore.ieee.org.

Digital Object Identifier 10.1109/JMEMS.2013.2266411

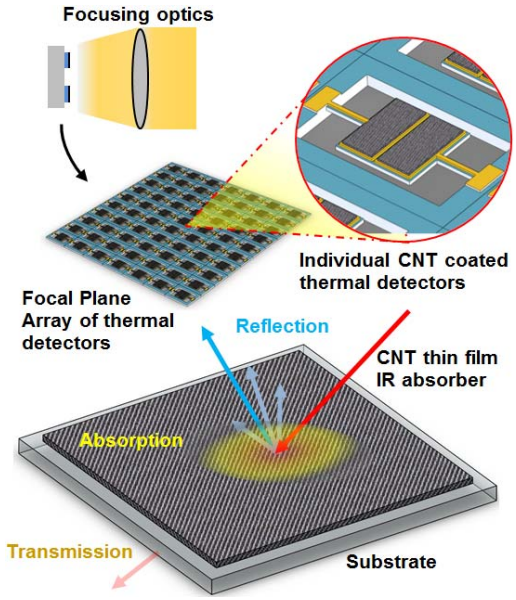

Fig. 1. A schematic showing one of the intended applications of the carbon nanotube/nanodiamond/polymer based coating: a focal plane array of resonant IR detectors [10]. Each array comprises of multiple thermal detector "pixels" that are individually addressed, forming an imaging system with high spatial resolution. The detectors are coated with the absorber layer, which efficiently converts the incident radiation into heat.

and ease of integration with electronics and microsystems makes this an attractive material for use in IR detectors and thermal energy harvesters (Fig. 1).

II. Experimental Results

A. Fabrication of CNT/DND/Polymer Nanocomposite

Researchers have previously fabricated horizontally dispersed CNT mats for infrared absorption using vacuum filtration [16]–[19] or airbrushing [20]. Neither method gives the desired combination of very thin films that are mechanically stable and can be further patterned or processed. In the procedure described in detail elsewhere [15] and summarized below, CNT powder is commercially purchased at low cost and mixed with a polymer (*i.e.* poly-(methylmethacrylate) (PMMA)) [21] in order to provide the eventual film with the required mechanical and thermal stability, and amenability to post-processing. In the spun layers of CNT/PMMA, the orientation of the CNTs is generally horizontal and follows no particular order, other than the strong tendency to agglomerate into bundles due to surface forces [8], [21], [22] (Figs. 2(a) and (b)). The agglomeration of CNTs in the polymer can be prevented by mixing surfactants to separate the CNT bundles. In this work, electrically charged DNDs are used as effective surfactants, counteracting the CNT agglomeration by electrostatic repulsion [22]. Unlike liquid surfactants, the DNDs are not volatile and remain in the film after spinning and baking. The DNDs used in this work have an average diameter of 30 nm and a ζ-potential of +45 mV. Ultrasonication aids with dispersing CNTs in the polymer by shearing the CNTs, but is largely ineffective without the DNDs. The final CNT/PMMA/DND layer is mechanically and thermally stable and can be spin coated on a substrate and patterned using standard photolithography and plasma etching.

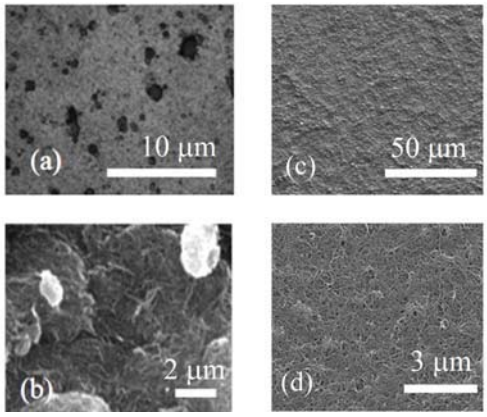

Fig. 2. (a), (b) Large agglomerates seen in the CNT/polymer films without the charged DND particles. (c) An SEM image of a thin film of CNT/DND in the PMMA matrix, showing that CNTs are stably enmeshed in the film with the addition of charged DNDs. (d) Magnified image of the same layer as (c), showing the grid like structure of the film.

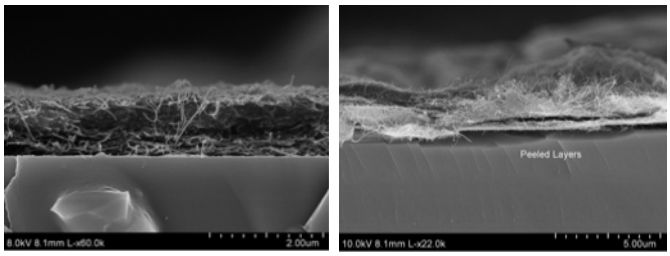

(a) (b)

Fig. 3. Cross section SEM images of a 1600 nm thick CNT composite film fabricated using 5 layers. (a) It is difficult to see the layers individually in a well meshed film. (b) When the film is slightly peeled away, the distinct layers can be seen more clearly.

Further addition of dimethylsulfoxide (DMSO) as a liquid surfactant helped with achieving lower viscosity and thus thinner films. For films having 0.6 w/v % DND and 0.2 w/v % CNT in DMSO, we were able to achieve excellent dispersion of the CNT films with surface roughness in the range of 50 to 100 nm [15], over a substrate size of 25 mm $\times$ 25 mm (Figs. 2(c) and (d)). This is in stark contrast to the large ($\sim$10 μm thick) agglomerates encountered prior to the addition of the DNDs (Fig. 2 (b)), and thus the addition of DNDs proved crucial to this process. With a low spin speed ($<$500 rpm), we were able to get consistent, visibly black films on a glass substrate, with a thickness on the order of 300 nm per layer. Following the spinning process, the films were baked on a hotplate at 110 °C to evaporate the DMSO solvent and cure the polymer. This bake step represents the maximum temperature used in this entire process. Multiple layers of the film can be sequentially deposited to increase the film thickness if needed (Fig. 3). The films discussed in further sections have multiple layers resulting in measured thicknesses of 1600 nm and 2000 nm (5 and 7 layers, respectively).

B. Infrared Absorption

To characterize the IR absorption properties of the CNT/DND based polymer, normal incidence reflection $R_{exp}(\lambda)$ and transmission $T_{exp}(\lambda)$ measurements are acquired on glass slides coated with the thin films using a Perkin

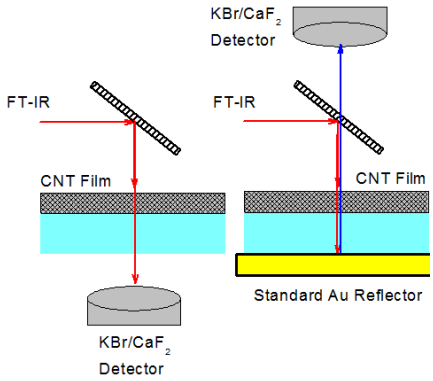

Fig. 4. A schematic of the normal incidence transmission and reflection test setup. The measurements are normalized using uncoated glass substrates for transmission and a standard gold reference for reflection.

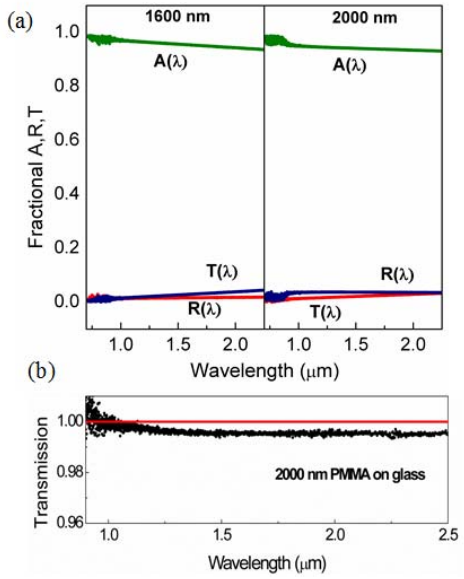

Fig. 5. (a) The reflection, transmission, and the absorption of the 1600 nm and 2000 nm films. (b) Transmission measurement for a 2000 nm thick layer of poly-methylmethacrylate (PMMA) on a glass substrate, indicating that the PMMA itself does not contribute significantly to the IR absorption.

Elmer Spectrum GX in the spectral range of 4000 cm^{-1} to 14 000 cm^{-1} with a spectral resolution of 4 cm^{-1}. Transmission measurements are normalized to an identical uncoated glass substrate, while reflection measurements are normalized to an uncoated glass substrate placed on a gold coated standard (Fig. 4) [23], [24]. Absorption for the film $A_{exp}(\lambda)$ is calculated as $A_{exp}(\lambda) = 1 - R_{exp}(\lambda) - T_{exp}(\lambda)$. Measured results for the two samples demonstrate a high broadband absorption (Fig. 5(a)). The effect of pure PMMA layers is considered (Fig. 5(b)) and measurements prove that it does not contribute significantly to the absorption.

C. Stability and Damage Resistance

With the inclusion of a polymer matrix, the films are fairly resistant to damage. They have endured some standard micromachining processes including evaporation/sputtering, liftoff, and some acid etches. The IR performance of the films does not change significantly after cycling at elevated temperatures (Fig. 6) and the films do not degrade perceptibly.

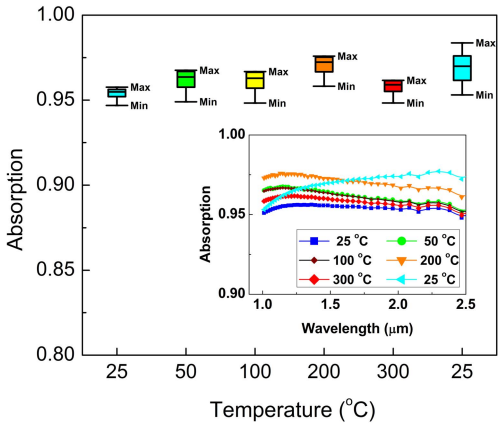

Fig. 6. Variation of absorption after thermal cycling of the 2000 nm film. The absorption characteristics are very reliable, with a standard deviation on the order of 1% across the measured spectral range even after heating the films up to 300 °C. No physical degradation of the film is observed. (Inset): Absorption in the NIR spectrum of the same film after thermal cycling.

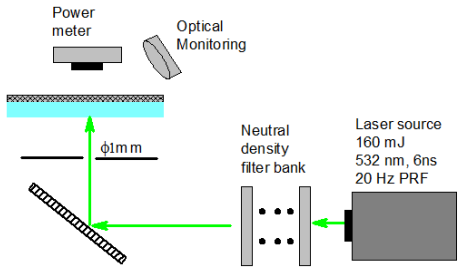

Fig. 7. Measurement setup for the estimation of the high power laser damage threshold, using a 532 nm, 6 ns pulsed laser source, multiple neutral density filters, and a power meter.

One of the main requirements of an absorber is to have stability at high irradiation powers. To study the laser damage resistance of the CNT/DND based polymers, preliminary testing has been carried out using a procedure similar to the one reported for gold black [25]. In this experiment, single 6 ns pulses from a 532 nm Nd:YAG laser with a 160 mJ output energy were irradiated onto the sample (Fig. 7). Spot diameter was maintained at 1 mm using a fixed aperture. Various input energy levels were obtained using neutral density filters with known attenuation. Most samples show some slight visible change above energy densities of 13 mJ/cm^2, and are completely ablated above 28 mJ/cm^2. Thus initial results shown in Fig. 8 indicate that these films have similar tolerances to gold black [25] and can be used as detector coatings in high power environments. More rigorous testing is necessary to verify the use of these films in laser radiometry.

III. Analysis

A. Extraction of Optical Parameters

Optical properties of ordered arrays of nanotubes can be analytically modeled [26]. However, because of the random dispersion of CNT/DNDs in the polymer, accurate modeling of the optical properties is challenging for the presented films. Instead, the optical constants are extracted from the

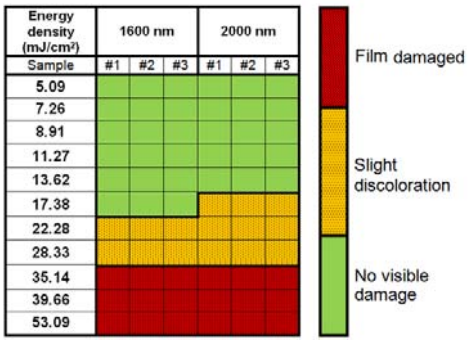

Fig. 8. A qualitative visual estimate of the onset of film damage upon irradiation with high power, fast laser pulses. Three samples each are measured for the two films. The damage threshold is estimated to be on the order of 28 mJ/cm^2.

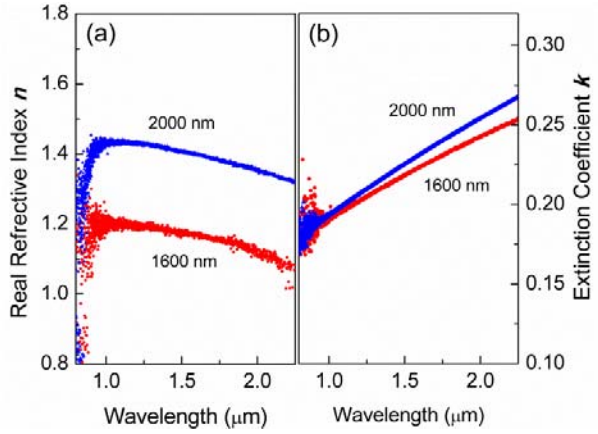

Fig. 9. (a) Extracted effective $\boldsymbol{n}$ for the measured films. (b) Extracted effective $\boldsymbol{k}$ for these films is more than 10 times higher than that for aligned CNT forests, resulting in increased absorption in a significantly lower thickness.

measured results using an effective media approximation. Measured results are compared to Heavens' model for normal incidence [27], which self-consistently relates $R_{exp}(\lambda)$ and $T_{exp}(\lambda)$ with the effective complex refractive index of the material $(\boldsymbol{n}-i\boldsymbol{k})$. For dominantly absorbing films, Heavens' relation can be approximated by the following system of equations [28].

$$T_{mod}(\lambda) = \frac{16 n_0 n_s \left(\boldsymbol{n}^2+\boldsymbol{k}^2\right)}{\left\{(\boldsymbol{n}+n_s)^2+(\boldsymbol{k}+k_s)^2\right\}\left\{(\boldsymbol{n}+n_0)^2+\boldsymbol{k}^2\right\}} e^{-\boldsymbol{\alpha}}, \quad (1)$$

$$R_{mod}(\lambda) = \frac{(n_0-\boldsymbol{n})^2+\boldsymbol{k}^2}{(n_0+\boldsymbol{n})^2+\boldsymbol{k}^2}, \quad (2)$$

$$\boldsymbol{\alpha}(\lambda) = \frac{4\pi \boldsymbol{k} d}{\lambda}, \quad (3)$$

where $\boldsymbol{n}$, $\boldsymbol{k}$, d, λ, $\boldsymbol{\alpha}$ describe the refractive index (real part), extinction coefficient, total film thickness, wavelength, and dimensionless attenuation of the thin film, respectively. The subscript ***mod*** refers to modeled values, while the subscripts ***s*** and ***0*** specify indices for the substrate and free space, respectively. As the measured results are normalized to the substrate, the calculation is effectively for a freely suspended CNT/DND/PMMA film [24]. A bivariate Newton-Rhapson method is used to fit the $(\boldsymbol{n}, \boldsymbol{k})$ values according to the iterative algorithm given by

$$\begin{bmatrix} T_{mod} \\ R_{mod} \end{bmatrix}_{p+1} = \begin{bmatrix} T_{mod} \\ R_{mod} \end{bmatrix}_{p} + \boldsymbol{J_p}^{-1} \begin{bmatrix} T_{exp} & -T_{mod} \\ R_{exp} & -R_{mod} \end{bmatrix}_{p}, \quad (4)$$

$$\boldsymbol{J_p} = \begin{bmatrix} \frac{\partial T_{mod}}{\partial \hat{k}^n_{mod}} & \frac{\partial R_{mod}}{\partial \hat{k}^n_{mod}} \\ \frac{\partial T_{mod}}{\partial k} & \frac{\partial R_{mod}}{\partial k} \end{bmatrix}_{p}. \quad (5)$$

The error between the modeled and measured results is given by $\left(\left(\boldsymbol{T_{mod}}-\boldsymbol{T_{exp}}\right)^2+\left(\boldsymbol{R_{mod}}-\boldsymbol{R_{exp}}\right)^2\right)^{\frac{1}{2}}$, and iteration is continued until error is reduced to 10^{-12}, guaranteeing a very precise fit. Extracted values for $(\boldsymbol{n}, \boldsymbol{k})$ from the two films are shown in Fig. 9(a) and Fig. 9(b), respectively. Solutions do not converge at the noisy edges of the measurement range close to 700 nm and 2400 nm.

Physically, the absorption in the film has significant contributions from scattering due to the many scattering centers provided by the well-dispersed CNTs with a diameter much smaller than the wavelength, as well as the intrinsic absorption provided by the CNTs. The small DND particles are not expected to contribute significantly to the optical absorption. These well-dispersed and dense films have at least an order of magnitude higher extinction coefficient $\boldsymbol{k}$ than vertically aligned CNT forests of the same thickness [4]. Increasing the density and improving the dispersion homogeneity of the CNTs in the matrix can further increase scattering and improve the effective extinction coefficient of the films. However, this could adversely impact the value of $\boldsymbol{n}$. It can be seen from Fresnel's equations that $\boldsymbol{n}$ should be as close to unity as possible to provide near-perfect index matching to the free space. The nature of the film surface poses some restrictions on index matching, leading to non-zero reflection. Reflections can be further suppressed by using a very thin anti-reflection coating on the nanocomposite.

A good comparison of the attenuation in the films is achieved by comparing the attenuation per unit thickness $(\boldsymbol{\alpha}/d)$ (Fig. 10(a)). Increasing the number of layers improves the absorption (Fig. 10(b)). When the film thickness reaches a value five times the optical penetration depth, more than 99% absorption is achieved and increasing the film thickness further does not change the $(\boldsymbol{\alpha}/d)$ ratio significantly [24]. This is consistent with the high absorbance in the 1600 nm and the 2000 nm films with penetration depths much less than the film thickness. The penetration depths of the films are simulated using COMSOL [29] and using the measured values for $\boldsymbol{n}$ and $\boldsymbol{k}$ as shown in Fig. 11. The inset of Fig. 11 shows the power absorbed in the suspended 2000 nm film, for normal incidence with two representative wavelengths of 600 nm and 2500 nm. The optical power absorbed in the layer manifests itself as a change in the temperature of the film, which is the desired result. The measured trend is consistent with the reported data, and measurements in the mid (3 μm–5 μm) and far IR (8 μm–14 μm) range for randomly dispersed CNT mats indicate that the penetration depths are on the order of 300 nm to 500 nm [18]. This makes it possible to realize thin film absorbers with $\geq$ 99% absorption and still maintain a profile below $\sim$2000 nm. As mentioned earlier, the film thickness can be further reduced to submicron levels by increasing the CNT density and reducing surface reflections using anti-reflection coatings.

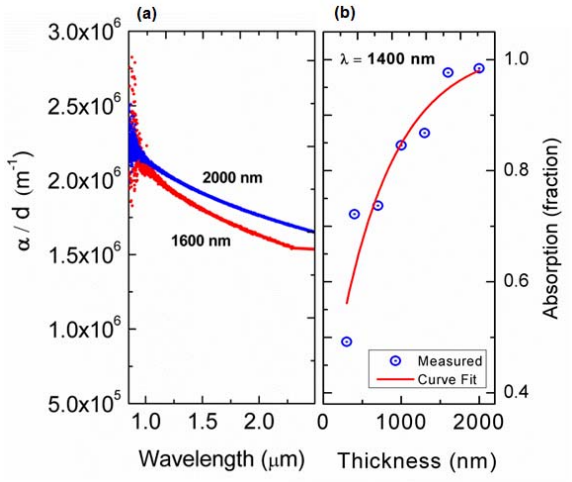

Fig. 10. (a) Measured attenuation per meter $\boldsymbol{\alpha}/\boldsymbol{d}$ of the films. The values are consistent with other published data on dispersed CNTs [18]. (b) Absorption as a function of film thickness at the representative NIR/SWIR wavelength of 1.4 μm.

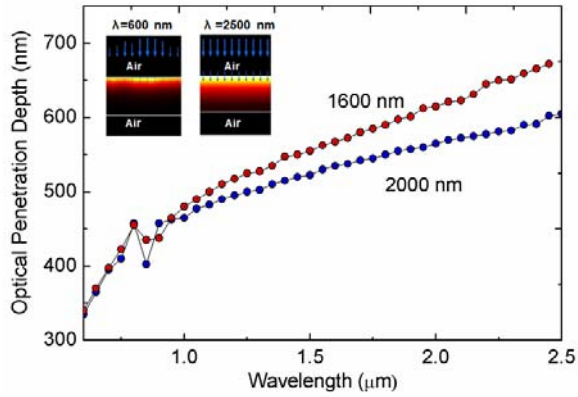

Fig. 11. Simulated optical penetration depth as a function of wavelength at normal incidence for the 1600 nm and 2000 nm thick CNT/PMMA/DND films. (Inset) Power absorbed in the suspended 2000 nm film, for normal incidence with two representative wavelengths of 600 nm and 2500 nm, showing the wavelength dependence of penetration depth. Blue arrows indicate time averaged power flow vectors.

B. Angular Dependence

Finite element simulations are used in order to verify the normal incidence measurements and extend the analysis to other angles. The COMSOL simulations agree with the measured data (Fig. 12), confirming that the effective media approximations can accurately describe the optical performance of the fabricated CNT-based nanocomposites.

As shown in Fig. 13, the films remain highly absorbing even at large incidence angles (θ_i), with the absorption efficiency greater than 90% at 45°, and greater than 80% at 60°. Only as θ_i approaches 85° the reflection overshadows the absorption (Fig. 13). The film is bi-axially symmetric in-plane and therefore, the TE and TM polarization yields similar results. The large range of acceptance angles with a very high absorbance makes this an especially attractive material for thermal detectors and energy harvesters.

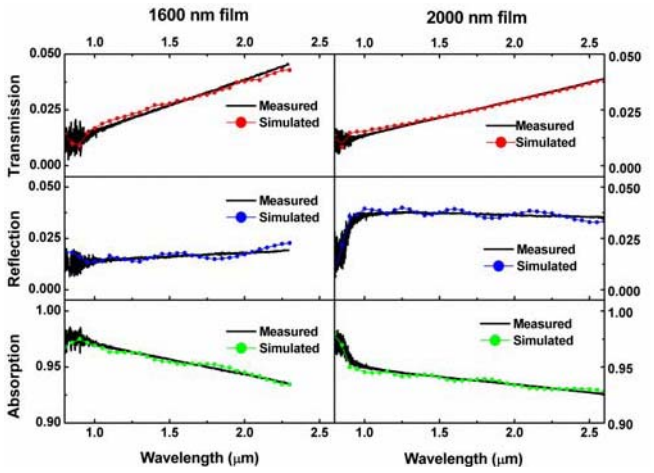

Fig. 12. Measured and simulated data for normal incidence for the 1600 nm and 2000 nm thick films, showing excellent agreement. This allows us to use the COMSOL model for further analysis. Simulated curves are identical for TE and TM modes because of the planar isotropy of the films.

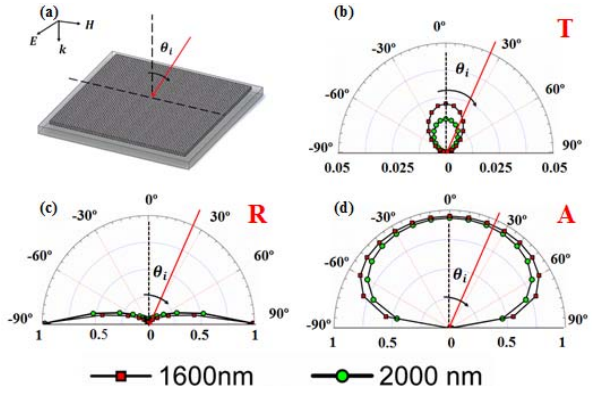

Fig. 13. (a) Angular incidence of radiation on the nanocomposite film, and the simulated dependence of (b) transmission, (c) reflection and (d) absorbance for the 1600 nm and 2000 nm thick films. Notice that transmission remains fairly low at all angles, whereas reflection dominates at high incident angles tending towards 90°. Consequently, the film retains its highly absorbing nature at most incident angles. The above graphs show values for a representative wavelength of 1 μm; simulations show a small dependence on the wavelength.

IV. Conclusion

The results presented in this work demonstrate the potential of CNT/DND based polymer films as efficient absorbers of NIR/SWIR radiation. The measured data indicate IR absorption comparable to thick vertical CNT arrays, but in a considerably thinner film. The addition of the polymer gives the film mechanical stability and makes it possible to pattern the film lithographically. Further work on this material can foreseeably improve attenuation per unit length by increasing the CNT volume fraction and improving the CNT dispersion, allowing submicron films that can absorb as efficiently. Rigorous investigation is also needed to characterize the thermal conductivity, heat capacity, and electrical characteristics of this class of materials as a function of the CNT fraction in the polymer.

The processing used for fabrication of these films is done at low temperatures and is compatible with other upstream and downstream micromachining processes, giving us the possibility to integrate these films into infrared sensors, focal

plane arrays, high optical power detectors, and microscale energy harvesters.

ACKNOWLEDGMENT

The authors thank Mr. Y. Sui for his help with fabrication, the staff at the Lurie Nanofabrication Facility for providing fabrication facility, the staff at the Analytical Instruments Laboratory of the Department of Chemistry for their help with IR measurements, and Dr. L. J. Guo and Mr. T. Lee, Department of Electrical Engineering and Computer Science, for access to the laser damage threshold experiment.

REFERENCES

[1] J. Lehman, A. Sanders, L. Hanssen, B. Wilthan, J. Zeng, and C. Jensen, "Very black infrared detector from vertically aligned carbon nanotubes and electric-field poling of lithium tantalate," *Nano Lett.*, vol. 10, pp. 3261–3266, Aug. 2010.

[2] N. Liu, M. Mesch, T. Weiss, M. Hentschel, and H. Giessen, "Infrared perfect absorber and its application as plasmonic sensor," *Nano Lett.*, vol. 10, pp. 2342–2348, Jul. 2010.

[3] J. Hendrickson, J. P. Guo, B. Y. Zhang, W. Buchwald, and R. Soref, "Wideband perfect light absorber at midwave infrared using multiplexed metal structures," *Opt. Lett.*, vol. 37, pp. 371–373, Feb. 2012.

[4] H. Shi, J. G. Ok, H. W. Baac, and L. J. Guo, "Low density carbon nanotube forest as an index-matched and near perfect absorption coating," *Appl. Phys. Lett.*, vol. 99, pp. 211103-1–211103-3, Nov. 2011.

[5] A. Rogalski, "Infrared detectors: Status and trends," *Progr. Quantum Electron.*, vol. 27, nos. 2–3, pp. 59–210, 2003.

[6] P. W. Kruse, *Uncooled Thermal Imaging: Arrays, Systems, and Applications*. Bellingham, WA, USA: SPIE, 2001.

[7] J. H. Lee, I. Bargatin, T. O. Gwinn, M. Vincent, K. A. Littau, R. Maboudian, Z.-X. Shen, N. A. Melosh, and R. T. Howe, "Microfabricated silicon carbide thermionic energy converter for solar electricity generation," in *Proc. IEEE 25th Int. Conf. MEMS*, Paris, France, Jan./Feb. 2012, pp. 1261–1264.

[8] M. Shossig, "Optical absorption layers for infrared radiation," in *Bio and Nano Packaging Techniques for Electron Devices*, G. Gerlach and K.-J. Wolter, Eds. Berlin, Germany: Springer-Verlag, 2012, pp. 355–381.

[9] G. K. Mor, S. Kim, M. Paulose, O. K. Varghese, K. Shankar, J. Basham, and C. A. Grimes, "Visible to near-infrared light harvesting in TiO_2 nanotube array-P3HT based heterojunction solar cells," *Nano Lett.*, vol. 9, pp. 4250–4257, Dec. 2009.

[10] V. J. Gokhale, Y. Sui, and M. Rais-Zadeh, "Novel uncooled detector based on gallium nitride micromechanical resonators," *Proc. SPIE*, vol. 8353, p. 835319, May 2012.

[11] W. Lang, K. Kuhl, and H. Sandmaier, "Absorbing layers for thermal infrared detectors," *Sens. Actuators A, Phys.*, vol. 34, pp. 243–248, Sep. 1992.

[12] R. J. C. Brown, P. J. Brewer, and M. J. T. Milton, "The physical and chemical properties of electroless nickel-phosphorus alloys and low reflectance nickel-phosphorus black surfaces," *J. Mater. Chem.*, vol. 12, pp. 2749–2754, Jul. 2002.

[13] K. Aydin, V. E. Ferry, R. M. Briggs, and H. A. Atwater, "Broadband polarization-independent resonant light absorption using ultrathin plasmonic super absorbers," *Nature Commun.*, vol. 2, p. 517, Nov. 2011.

[14] K. Mizuno, J. Ishii, H. Kishida, Y. Hayamizu, S. Yasuda, D. N. Futaba, M. Yumura, and K. Hata, "A black body absorber from vertically aligned single-walled carbon nanotubes," *Proc. Nat. Acad. Sci. USA*, vol. 106, pp. 6044–6047, Apr. 2009.

[15] Y. Sui, V. J. Gokhale, O. A. Shenderova, G. E. McGuire, and M. Rais-Zadeh, "A thin-film infrared absorber using CNT/nanodiamond nanocomposite," *MRS Proc.*, vol. 1452, pp. 1–6, May 2012.

[16] C. Koechlin, S. Maine, S. Rennesson, R. Haidar, B. Tretout, J. Jaeck, N. Péré-Laperne, and J.-L. Pelouard, "Potential of carbon nanotubes films for infrared bolometers," *Proc. SPIE*, vol. 7945, pp. 794521-1–794521-8, Jan. 2011.

[17] P. Merel, J. B. A. Kpetsu, C. Koechlin, S. Maine, R. Haidar, J. L. Pelouard, A. Sarkissian, M. I. Ionescu, X. Sun, P. Laou, and S. Paradis, "Infrared sensors based on multi-wall carbon nanotube films," *Comptes Rendus Phys.*, vol. 11, pp. 375–380, Jul. 2010.

[18] S. Maine, C. Koechlin, S. Rennesson, J. Jaeck, S. Salort, B. Chassagne, F. Pardo, J.-L. Pelouard, and R. Haïdar, "Complex optical index of single wall carbon nanotube films from the near-infrared to the terahertz spectral range," *Appl. Opt.*, vol. 51, pp. 3031–3035, May 2012.

[19] Á. Kukovecz, R. Smajda, M. Oze, H. Haspel, Z. Kónya, and I. Kiricsi, "Pyroelectric temperature sensitization of multi-wall carbon nanotube papers," *Carbon*, vol. 46, pp. 1262–1265, Aug. 2008.

[20] J. H. Lehman, K. E. Hurst, A. M. Radojevic, A. C. Dillon, and R. M. Osgood, Jr., "Multiwall carbon nanotube absorber on a thin-film lithium niobate pyroelectric detector," *Opt. Lett.*, vol. 32, pp. 772–774, Apr. 2007.

[21] A. Martinez, S. Uchida, Y.-W. Song, T. Ishigure, and S. Yamashita, "Fabrication of carbon nanotube-poly-methylmethacrylate composites for nonlinear photonic devices," *Opt. Exp.*, vol. 16, pp. 11337–11343, Jul. 2008.

[22] S. C. Hens, G. Cunningham, G. McGuire, and O. Shenderova, "Nanodiamond-assisted dispersion of carbon nanotubes and hybrid nanocarbon-based composites," *Nanosci. Nanotechnol. Lett.*, vol. 3, pp. 75–82, Feb. 2011.

[23] X. J. Wang, J. D. Flicker, B. J. Lee, W. J. Ready, and Z. M. Zhang, "Visible and near-infrared radiative properties of vertically aligned multi-walled carbon nanotubes," *Nanotechnology*, vol. 20, no. 21, p. 215704, May 2009.

[24] H. Ye, X. J. Wang, W. Lin, C. P. Wong, and Z. M. Zhang, "Infrared absorption coefficients of vertically aligned carbon nanotube films," *Appl. Phys. Lett.*, vol. 101, no. 14, pp. 141909-1–141909-4, Oct. 2012.

[25] J. Lehman, E. Theocharous, G. Eppeldauer, and C. Pannell, "Gold-black coatings for freestanding pyroelectric detectors," *Meas. Sci. Technol.*, vol. 14, pp. 916–922, Jul. 2003.

[26] F. J. Garcia-Vidal, J. M. Pitarke, and J. B. Pendry, "Effective medium theory of the optical properties of aligned carbon nanotubes," *Phys. Rev. Lett.*, vol. 78, pp. 4289–4292, Jun 1997.

[27] O. S. Heavens, *Optical Properties of Thin Solid Films*. London, U.K.: Butterworth, 1955.

[28] S. G. Tomlin, "Optical reflection and transmission formulae for thin films," *J. Phys. D, Appl. Phys.*, vol. 1, no. 12, pp. 1667–1671, 1968.

[29] *COMSOL* [Online]. Available: http://www.comsol.com

Vikrant Jayant Gokhale (S'10) received the B.Tech. degree in electronics and instrumentation engineering from the Vellore Institute of Technology, Tamil Nadu, India, and the M.S. degree in electrical and computer engineering from the University of Michigan, Ann Arbor, MI, USA, in 2007 and 2010, respectively.

He is currently a doctoral candidate in electrical engineering at the University of Michigan. From 2007 to 2008, he was an Engineer at Honeywell Technology Solutions, Sensing and Control, Bangalore, India. His current research interests include MEMS sensor design and fabrication, GaN resonators resonant infrared detectors, carbon nanotube based nanocomposites, and acoustoelectric effect.

Olga A. Shenderova received the Ph.D. degree in materials science from St. Petersburg State Technical University, St. Petersburg, Russia, in 1991.

She is President of Adámas Nanotechnologies, Inc., Raleigh, NC, USA, and the Head of the Nanocarbon Laboratory, International Technology Center (ITC), Raleigh. Since 2001, she has worked at ITC on applied research projects in the areas of nanodiamond (ND) particle surface modification, influence of synthesis conditions on ND composition, nitrogen state in ND, development of ND-based additives for lubricants, ND-polymer composites, and optical and biological applications of ND. She started Adámas Nanotechnologies, Inc for the commercialization of nanodiamond particles and related technologies. She has given more than 100 invited talks and authored over 120 papers in peer-reviewed journals, 15 book chapters, and edited five books related to nanodiamonds. She has published 20 patents.

Gary E. McGuire received the Ph.D. degree in inorganic chemistry from the University of Tennessee, Knoxville, TN, USA, in 1972.

He is the President of the International Technology Center, a non-profit research center, Research Triangle Park, NC, USA. Program areas of current interest include terahertz electronics, atmospheric pressure plasmas, nanodiamond and related nanocomposite materials, infrared optics, and thermal interface materials. Historically, his interests include the development and characterization of new materials and processes for novel semiconductor devices stemming from his early career at Texas Instruments.

Dr. McGuire is the Past-Editor of the *Journal of Vacuum Science and Technology B*. He has published over 130 articles and 35 books and book chapters for which he served as the senior author or editor and has 19 patents to his name.

Mina Rais-Zadeh (S'03–M'08–SM'12) received the B.S. degree in electrical engineering from Sharif University of Technology, Tehran Iran, and the M.S. and Ph.D. degrees in electrical and computer engineering from the Georgia Institute of Technology, Atlanta, GA, USA, in 2005 and 2008, respectively.

From August 2008 to 2009, she was a Post-Doctoral Research Fellow with the Integrated MEMS Group, Georgia Institute of Technology. Since January 2009, she has been with the University of Michigan, Ann Arbor, MI, USA, where she is currently an Assistant Professor in the Department of Electrical Engineering and Computer Science.

Dr. Rais-Zadeh was a recipient of the NSF CAREER Award in 2011, the IEEE Electron Device Society Early Career Award in 2011, and the NASA Early Career Faculty Award in 2012. She was the finalist in student paper competitions at the SiRF conference in 2007 and IMS conference in 2011. She is the chairperson of the Display, Sensors and MEMS Sub-Committee at the 2013 IEEE International Electron Devices Meeting (IEDM). She has served as a member of the technical program committees of IEEE IEDM, IEEE Sensors Conference, and the Hilton Head Workshop. Her current research interests include RF MEMS, passive micromachined devices for communication applications, resonant micromechanical devices, gallium nitride MEMS, and micro/nano fabrication process development.